SPATIALLY-RESOLVED NIR SPECTRAL EFFECTS OF SPACE WEATHERING IN LUNAR PLAGIOCLASE K. L. Utt[1], R. C. Ogliore[1], B. L. Jolliff[2], H. A. Bechtel[3], J. J. Gillis-Davis[1]. [1]Department of Physics, Washington University in St. Louis, St. Louis, MO 63130, USA, [2]Department of Earth and Planetary Sciences, Washington University in St. Louis, St. Louis, MO 63130, USA, [3]Advanced Light Source Division, Lawrence Berkeley National Laboratory, Berkeley, California 94720, USA (Correspondence: k.l.utt@wustl.edu)

Introduction: Space-exposed lunar soil grains are subject to micrometeoroid impacts and solar wind bombardment, a process broadly described as "space weathering." The spectral effect of space weathering on lunar soils — darkening, reddening, and loss of spectral contrast — has been largely attributed to the formation and accumulation of nanophase iron (npFe^0) particles in amorphous rims ($<$200 nm) coating mineral grains [1, 2, 3, 4]. While it is possible to study npFe^0 within the amorphous rim via transmission electron microscopy, previous infrared (IR) spectroscopic studies have been limited to bulk, far-field measurements due to the long wavelength of IR light. The recent development of near-field IR spectroscopic techniques with a spot size of 10–20 nm, however, provides the opportunity to collect spectra with nanoscale spatial resolution [5].

Here we report near-field IR spectral measurements in two cross-sections of a space-exposed lunar plagioclase grain. Both samples were collected from the same grain but were chosen such that we could investigate the effects of micrometeoroid impact and solar wind irradiation separately. The technique used for this study provides spatial resolution on the order of space weathering effects, whereas typical laboratory spectra and remote sensing data can only measure the bulk properties of the soil. Hence, with this technique, we can assess the IR spectral features of the individual components which comprise the spectra measured by bulk methods. With a more detailed understanding of the spectral effects of charged-particle irradiation on mineral and soil grains, it may also be possible to draw parallels to silicate processing in the interstellar medium [6].

Sample Preparation: Using an FEI Quanta 3D Focused Ion Beam (FIB), we extracted two targeted liftouts from a space-exposed region of a ∼250-µm grain from mature lunar soil 79221 [3]. SEM-EDS measurements collected with a Tescan Mira3 FEG-SEM (at 15 kV) indicate that the grain's composition is consistent with anorthite-rich plagioclase, consisting primarily of Si (16 at.%), Al (16 at.%), Ca (8 at.%), and O (60 at.%). A ∼3 µm protective Pt cap was deposited on the surface of the regions of interest before FIB sectioning.

One liftout (sample 1) was taken from a hypervelocity micrometeoroid impact crater (Fig. 1a). A second liftout (sample 2) was taken from a region of the space-exposed surface that included vesiculated and non-vesiculated melt splash and an adhering grain (Fig. 1b). The liftouts were thinned to a width of approximately 1 µm, polished with a low-kV ion beam, and placed on a Si chip with surface roughness $<$0.5 nm.

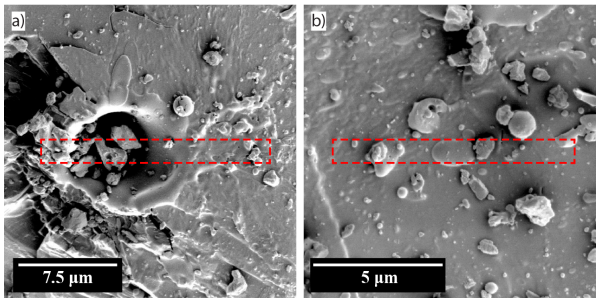

Figure 1: Secondary electron (SE) images (2 kV) showing grain surface from which a) sample 1 and b) sample 2 were extracted via FIB.

Methods: Using Synchrotron Infrared Nano Spectroscopy (SINS) at Beamline 5.4 at the Advanced Light Source [5], we collected spatially-resolved (spot size ∼20 nm) near-field IR (2-14 µm) attenuated total reflectance (ATR) spectra at various distances from the space-exposed surface of the samples. In total, we obtained five line scans (three from sample 1 and two from sample 2) comprised of 32 points, each separated by 60–120 nm, beginning below the surface of the sample and ending on the protective Pt cap. Background spectra were collected from the Pt cap periodically. All spectra shown in Fig. 2 and Fig. 3 are normalized to these Pt background scans.

Results: For sample 1 (Fig. 2a), we collected spectra with 4 cm^{-1} spectral resolution from points separated by 70 nm. A representative subset of the 18 spectra obtained from sample 1 is shown in Fig. 2c. Spectra from sample 2 (Fig. 3a) were collected with 8 cm^{-1} spectral resolution from points separated by 90 nm. A representative subset of the 22 spectra obtained from sample 1, with particular attention paid to points near the surface, is shown in Fig. 3c. Dots of the corresponding color in Fig. 3b and Fig. 2b indicate the points from which we collected the spectra.

Discussion: The spectra obtained from both samples were found to change with depth from the space-exposed grain surface in a manner consistent with space weathering [7, 8]. Relative to those collected further below the surface of either sample, the spectra collected near the surface of the same sample are characterized by loss of spectral contrast, preferential loss of intensity in short wavelengths, and reduced overall inten-

sity (darkening). While sample 1 and sample 2 produced spectra with qualitatively different features, spectra collected near the surface of both samples contain a broad feature in the 10–11 µm region whereas spectra collected further from the surface of both samples contain more distinct peaks in the same region. Although scans from both samples show depth-dependent darkening and broadening of spectral features, only scans from sample 2 were found to redden as we approached the surface. This discrepancy may be explained by impact-induced alteration of the crystal structure near the crater. Importantly, we did not observe any evidence of impactor residue in the microcrater, though there may be a thin (∼100 nm) layer of amorphized grain material along the crater surface.

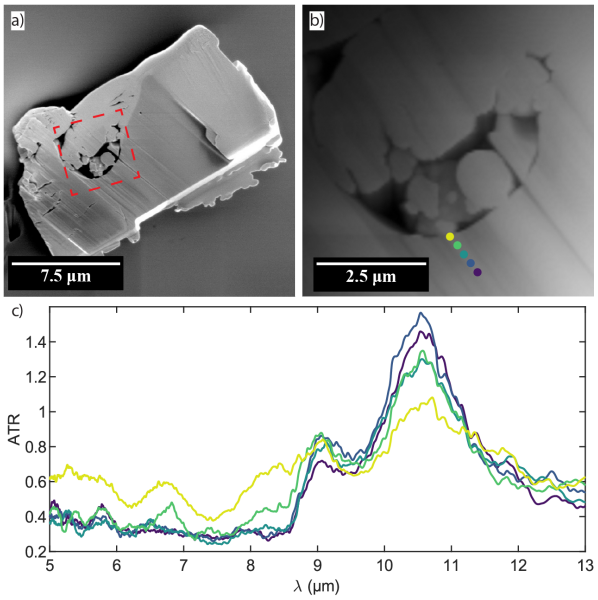

Figure 2: a) SE (2 kV) image of sample 1. b) AFM image (scanned area in dashed square) with locations of shown spectra. c) ATR spectra for each point, where purple is in the subsurface and yellow is the surface.

Collecting spatially-resolved point spectra at incremental distances from the space-exposed surface of the grain provides insight into the spectral changes that occur as a result of space weathering via solar wind irradiation and micrometeoroid impact-induced shock. These scans provide a snapshot of how the IR spectra of unexposed (less weathered) anorthite-rich lunar plagioclase changes due to exposure to solar wind and micrometeoroid impacts. Given that lunar soils exposed to solar wind display amorphous layers ∼60–200 nm thick [9], we are confident that we collected spectra over a range of depths sufficient to capture these changes.

Future Work: In future studies, we plan to perform coordinated SINS and TEM measurements in order to understand the relationship between the spectral

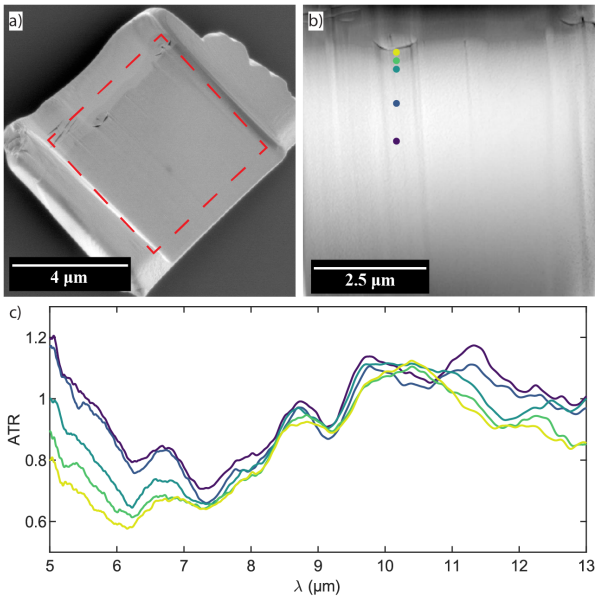

Figure 3: a) SE (2 kV) image of sample 2. b) AFM image (scanned area in dashed square) with locations of shown spectra. c) ATR spectra for each point, where purple is in the subsurface and yellow is the surface.

and crystallographic changes caused by space weathering. Such coordinated measurements may also shed light on compositional or physical variations among and between samples. We will also collect spectra from plagioclase, olivine, and other relevant mineral standards prepared identically to our samples, which should allow for a better understanding of any instrumental artifacts and help explain the observed discrepancies between samples. We also hope apply these studies to the Diviner observations that Christiansen Feature values shift to longer wavelengths with increasing maturity [10].

Acknowledgments: This research used resources of the Advanced Light Source, which is a DOE Office of Science User Facility under contract no. DE-AC02-05CH11231. The spectral data were collected using the SINS instrument at beamline 5.4 at the ALS.

References: [1] C. M. Pieters et al. *JGR* 98.E11 (1993), 20817. [2] C. M. Pieters et al. *MAPS* 35.5 (2000), 1101–1107. [3] L. A. Taylor et al. *JGR: Planets* 106.E11 (2001), 27985–27999. [4] S. K. Noble, L. P. Keller, and C. M. Pieters. *MAPS* 40.3 (2005), 397–408. [5] H. A. Bechtel et al. *PNAS (USA)* 111.20 (2014), 7191–7196. [6] J. E. Chiar and A. G.G. M. Tielens. *APJ* 637.2 (2006), 774–785. [7] B. Hapke. *JGR: Planets* 106.E5 (2001), 10039–10073. [8] S. K. Noble, C. M. Pieters, and L. P. Keller. *Icarus* 192.2 (2007), 629–642. [9] L. P. Keller and D. S. McKay. *GCA* 61.11 (1997), 2331–2341. [10] B. T. Greenhagen et al. *Science* 329.5998 (2010), 1507–1509.